Mon. Not. R. Astron. Soc. **000**, 000–000 (0000) Printed 2 February 2008 (MN LATEX style file v1.4)

On the environmental dependence of halo formation

Ravi K. Sheth[1] & Giuseppe Tormen[2]
[1] *Department of Physics & Astronomy, University of Pittsburgh, 3941 O'Hara Street, PA 15260, USA*
[2] *Dipartimento di Astronomia, Vicolo dell'Osservatorio 2, 35122 Padova, Italy*
Email: rks12@pitt.edu, tormen@pd.astro.it

Submitted to MNRAS 12 November 2003

ABSTRACT
A generic prediction of hierarchical gravitational clustering models is that the distribution of halo formation times should depend relatively strongly on halo mass, massive haloes forming more recently, and depend only weakly, if at all, on the large scale environment of the haloes. We present a novel test of this assumption which uses the statistics of weighted or 'marked' correlations, which prove to be particularly well-suited to detecting and quantifying weak correlations with environment. We find that close pairs of haloes form at slightly higher redshifts than do more widely separated halo pairs, suggesting that haloes in dense regions form at slightly earlier times than do haloes of the same mass in less dense regions. The environmental trends we find are useful for models which relate the properties of galaxies to the formation histories of the haloes which surround them.

Key words: galaxies: clustering – cosmology: theory – dark matter.

1 INTRODUCTION

The excursion set model of hierarchical clustering (Epstein 1983; Bond et al. 1991) has been remarkably successful. It provides useful analytic approximations for the abundance of haloes of mass m at time t (Bond et al. 1991; Sheth, Mo & Tormen 2001), for the conditional mass function of m haloes at t which are later (at $T > t$) in more massive haloes $M > m$ (Bond et al. 1991; Lacey & Cole 1993; Sheth & Tormen 2002), for the abundance of haloes as a function of the larger scale environment (Mo & White 1996; Lemson & Kauffmann 1999; Sheth & Tormen 2002) for the distribution of halo formation times (Lacey & Cole 1993) and masses (Nusser & Sheth 1999; Sheth & Tormen 2004). Here, formation is typically defined as that time when the most massive progenitor contains at least half the final mass.

In the simplest and most used approximation, this approach ignores most correlations between different spatial scales. In this approximation, the approach predicts that there should be no correlation between halo formation and the large scale environment in which the halo sits (White 1996). This is because, in the model, formation refers to a smaller mass than the final virial mass, and hence to a smaller spatial scale than that associated with the Lagrangian radius of an object, whereas the larger scale environment, by definition, refers to scales which are larger than that of the halo.

Lemson & Kauffmann (1999) presented evidence from measurements in numerical simulations of clustering that halo formation times were indeed independent of environment. They interpreted this as evidence that the excursion set neglect of correlations was justified. (Lemson & Kauffmann also presented evidence that a number of other physical properties of haloes were also independent of environment, and this evidence has been used to justify an assumption which enormously simplifies semi-analytic models of galaxy formation: that the properties of galaxies are determined by the haloes in which they form, and not by the surrounding larger-scale environment.) Their conclusion is somewhat surprising for the following reason. It is quite well established that the ratio of massive to low mass haloes is larger in dense regions, and that the excursion set model is able to quantify this dependence quite well (see the references given earlier). It is also well established that, on average, low mass haloes form at higher redshifts (see references given earlier). Together, these suggest that if one averages over the entire range of halo masses in any given region, then the mean formation time in dense regions should be shifted to lower redshifts, simply because these regions contain more massive haloes which, on average, form later. In Figure 4 of their paper, Lemson & Kauffmann averaged over the entire range of halo masses accessible to them in their simulations, and found no dependence of formation time on environement; at face value, this is *in*consistent with the simplest excursion set prediction!

The main goal of this paper is to repeat the test for environmental effects on halo formation. Section 2 shows that a simple plot of formation time versus local density does not show strong trends, suggesting that the excursion set approximation is rather accurate. But then, Section 3 presents

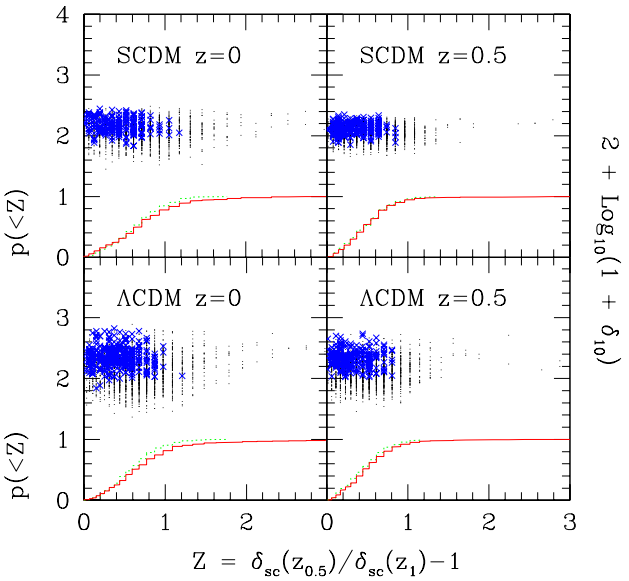

Figure 1. Joint distribution of halo formation times and environments. Crosses and dots represent massive and low mass haloes respectively. Histograms show the cumulative distribution of formation redshifts, averaged over the entire halo population, for two bins in density (dotted/solid curves show results for low/high densities). Although the symbols appear to show that low mass haloes in dense regions tend to have formation times which extend to higher redshifts, when averaged over the entire population of high- and low-mass haloes, there are no significant trends with environment.

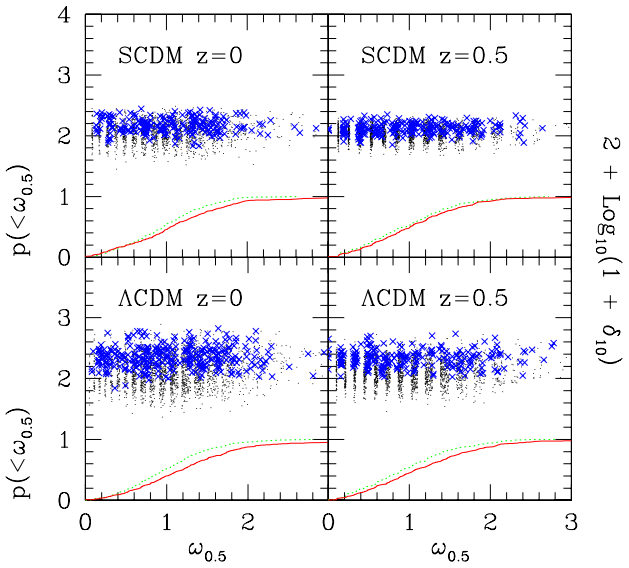

Figure 2. Same as previous figure, but now with scaled formation redshifts. Note that, in these scaled units, all haloes span the same range along the x-axis, whatever their mass. Histograms show the cumulative distribution of $\omega_{0.5}$, averaged over the entire halo population, for different bins in density (dotted/solid line is for lower/higher density environments). Comparison of the dotted and solid lines indicates that haloes in dense regions tend to have formation times which extend to higher redshifts compared to their counterparts in less dense regions.

evidence, from what we feel is a more senstive test, which indicates that low mass haloes in dense environments form slightly earlier than haloes of the same mass in less dense environments. Thus, it may be that, when one averages over a range of halo masses, the shift to later formation times associated with the fact that the dense regions contain the most massive haloes is approximately compensated-for by a density-dependent shift to slightly earlier formation times, with haloes in denser regions having larger formation redshifts than their counterparts (of the same mass) in the field. This second test uses a technique known as marked correlation functions: our results indicate that marked correlation functions are a powerful means of detecting and quantifying environmental dependences. Section 4 illustrates that our results do not depend sensitively on what definition of halo formation we use. A final section summarizes our findings, and argues that our results may have important implications for studies of halo structure. It also presents evidence which suggests that the density profiles of close halo pairs are neither more nor less centrally concentrated than are the profiles of their counterparts in less dense regions.

2 FORMATION TIMES AND ENVIRONMENT

We have identified the formation times of all haloes which contain more than two hundred particles in the GIF simulations of Kauffmann et al. (1999). These simulations are a subset of those made available to the public by the Virgo consortium (Frenk et al. 2000). Particle positions and velocities from the simulations were output at a range of redshifts, approximately evenly spaced in logarithmic expansion factor: $\Delta \ln(1+z) \approx 0.0596$. For each output time, we identified haloes using the spherical overdensity method (e.g. Lacey & Cole 1994; Tormen, Moscardini & Yoshida 2003) which contained at least twenty particles. The required overdensity is a cosmology dependent factor times the background density, as specified by the spherical collapse model. For the SCDM model, this factor is 178, and it is independent of redshift; for the ΛCDM model, it is 323 at $z = 0$, and is smaller at higher redshifts (e.g. Peebles 1993). At any given output time z_1, we selected the halos which were composed of more than two hundred particles, and studied the formation times and masses at formation of these haloes as follows. (For reference, an M_* halo at $z = 0$, 0.5 and 1.0 has 1289, 170 and 31 particles in the SCDM run, and 807, 185 and 40 particles in the ΛCDM run, so the high redshift runs mainly probe the formation times and masses of objects much larger than M_*.)

Given a halo of mass M_1 (i.e., containing N_1 particles) at z_1, we go to the previous output time ($z_1+\mathrm{d}z_2$, say), identify the object which contributes the most number of particles to N_1, and call it the most massive progenitor at $z_1+\mathrm{d}z_2$. Suppose this most massive progenitor had N_2 particles. We then go to the preceding output step ($z_1 + \mathrm{d}z_2 + \mathrm{d}z_3$, say) and identify the most massive progenitor, N_3, of N_2. We continue in this way until the number of particles in the most massive progenitor first falls below $N_1/2$. If the mass just

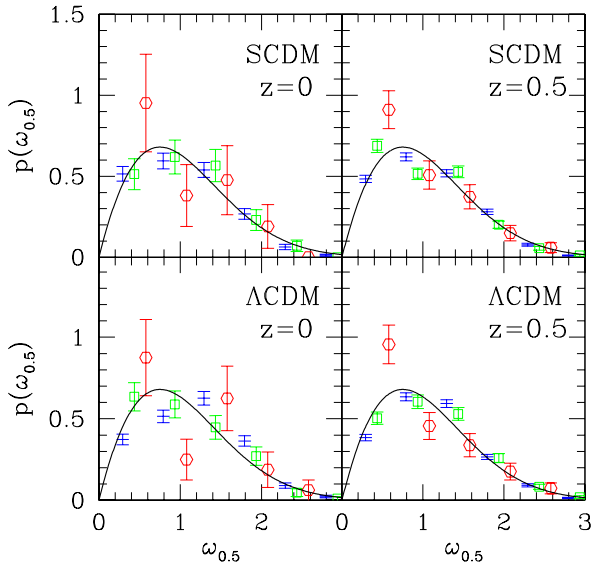

Figure 3. Distribution of scaled formation times. Panels on the left and right show results for parent halos identified at $z = 0$ and $z = 0.5$, and the different symbols in each panel show the distribution of scaled formation times for halos with masses in the range $1 < M/M_*(z) \leq 2$ (horizontal bars), $4 < M/M_*(z) \leq 8$ (squares),and $16 < M/M_*(z) \leq 32$ (hexagons). Solid line shows the expression derived by Lacey & Cole (1993).

before formation is N_n, then the mass just after formation is N_{n-1}, and the redshift of formation is $z_1 + \cdots + \mathrm{d}z_{n-1}$. We store these values for each halo M_1 at z_1.

In what follows, we use z_1 to denote the redshift at which the parent object is identified as a virialized halo, and $z_{0.5} > z_1$ to denote the redshift at which it formed (recall formation is when the object is one-half its final mass). To estimate the local environment of a halo, we have measured the mass in spheres of radius $R = 5$ and $10h^{-1}$ Mpc centred on the halo. We then define the local overdensity on scale R as $\delta_{\rm R} = M_{\rm R}/(\bar{\rho}\, 4\pi R^3/3) - 1$. We find qualitatively similar results for both δ_5 and δ_{10} (the main difference being that $\delta_5 \sim 10\delta_{10}$), so in what follows, we only show results for δ_{10}.

Figure 1 shows the joint distribution of halo formation redshifts and local densities δ_{10} (for clarity, we have shifted the estimate of the density upwards by 2 orders of magnitude, as indicated by the axis label on the right). The top panels show measurements for parent haloes identified in an SCDM simulation at $z = 0$ (left) and $z = 0.5$ (right), and the bottom panels show measurements in a ΛCDM simulation. In all panels, dots show results for low mass haloes (the subset with $0.25 < M/M_* < 0.5$ and $1 < M/M_* < 2$ for $z_1 = 0$ and 0.5, respectively), and crosses represent massive haloes ($M/M_* > 4$ and $M/M_* > 16$ for $z_1 = 0$ and 0.5).

The figure shows clearly that the most massive haloes do not populate the least dense cells, and that they do not form at early times. The dotted and solid histograms in the bottom of each panel show the cumulative distribution of formation times, averaged over all halo masses (i.e., not just the ones shown by the dots and crosses), in low and high density regions. This was done by first sorting all haloes by their local density, and then choosing those whose local density was in the lowest ten percent to make the dotted curves, and haloes whose local density was in the highest ten percent to make the solid curves. The similarity of the cumulative distributions suggests that there is little evidence for dependence of formation time on local density. This is essentially what Lemson & Kauffmann (1999) found, using a similar technique. (In fact, Lemson & Kauffmann defined the environment of a halo slightly differently—they use the density in a shell within $2h^{-1}$ and $5h^{-1}$Mpc of each halo, whereas we include the central region as well. Since most halos are smaller than $2h^{-1}$Mpc, our definition of local density places massive haloes in denser regions than does theirs.) Note, however, that as a result of the average over masses, this plot is difficult to interpret.

A slightly more straightforward plot to interpret is shown in Figure 2, were we have scaled all the formation times to $\omega_{0.5} = [\delta_{\rm sc}(z_{0.5}) - \delta_{\rm sc}(z_1)]/[\sigma^2(M/2) - \sigma^2(M)]^{1/2}$; in this variable, the dependence of formation time on mass has been removed (Lacey & Cole 1993). Comparison with the previous figure shows that, indeed, haloes of all masses now span the same range along the x-axis. Figure 3 shows this explicitly: the different symbols show the scaled formation time distribution for different halo populations in the simulations. The solid curves in each panel all show the same functional form, $p(\omega) = 2\omega\,\mathrm{erfc}(\omega/\sqrt{2})$. Notice that this functional form provides a reasonably good description of the scaled halo formation times over a wide range of masses and times. This rescaling allows us to look for a dependence on environment in the following sense: do haloes of a given mass in dense regions form at different times relative to their counterparts of the same mass in the field? The slight separation between the cumulative histograms indicates that there is marginal evidence for higher formation redshifts in dense regions.

Rather than quantifying this with a KS test, we have chosen to present the results of a different test which we believe is to be preferred, as it does not depend on the vagueries of what scale one chooses to define the local density (what is special about $10h^{-1}$Mpc? why make a spherical average? what if one excises the region occupied by the halo itself when estimating the local density?), or on how the choice of density threshold affects the result (how do the cumulative histograms change if we simply split the sample into two equal-sized halves, rather than compare only the extreme ends of the density distribution?).

3 A MARKED CORRELATION FUNCTION ANALYSIS

This section describes the results of a novel test of environmental effects on halo formation times: an analysis of the 'marked' correlations of the halo population, with formation time as the 'mark'. Let m_i and m_j denote the values of the marks associated with objects i and j, and let $\bar{m}$ denote the mean value of the mark, when averaged over all objects. The marked correlation function we will use, $M(r)$, is defined as the sum over all pairs with separations $r_{ij} = r$, weighted by the product of the marks $m_i m_j$, divided by the sum over the same pairs (i.e., those separated by r), but this time weighted by $\bar{m}^2$. In essence, $M(r)$ tests if pairs separated by

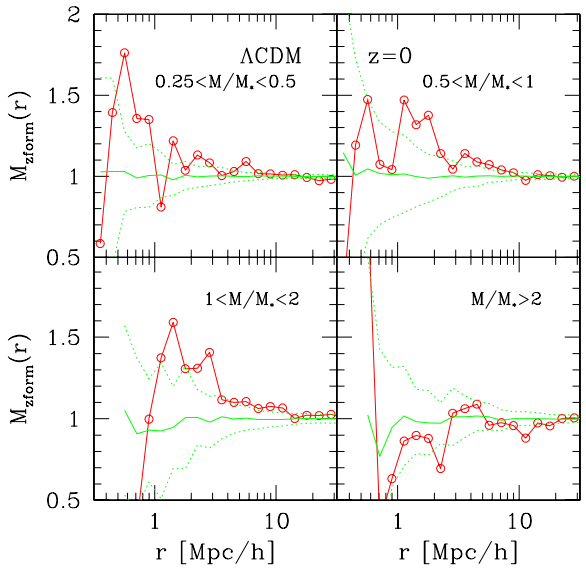

Figure 4. Marked correlation function, with formation time as the mark, for haloes identified at $z = 0$ in the ΛCDM simulation. Different panels show results for haloes of different masses. Symbols show the measurement, and dotted line shows the typical variation from the mean, shown as the heavy solid line, estimated by computing $M(r)$ from a randomized set of marks, and repeating one hundred times.

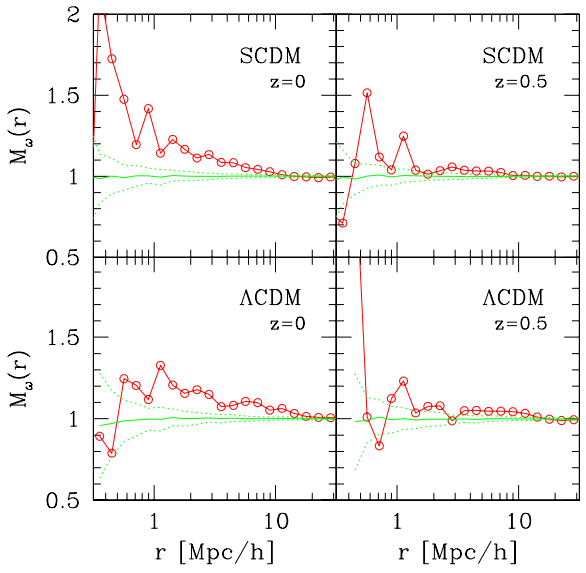

Figure 5. Same as previous figure, but now with scaled formation redshift as the mark. All panels show clear evidence for that close pairs tend to have larger formation redshifts.

r tend to have larger or smaller values than the mean mark. If we use the formation redshift as the mark, then a plot of $M(r)$ versus r shows if close pairs tend to have smaller ($M(r) < 1$) or larger ($M(r) > 1$) formation redshifts than average.

The previous section showed that halo formation times depend on mass. Since the clustering of haloes depends on their mass, an analysis which averages over a large range in halo masses will be difficult to interpret. Therefore, the different panels in Figure 4 show the marked correlation functions for a number of small bins in mass in the ΛCDM simulation at $z_1 = 0$. Results for other z_1 and for the SCDM model are qualitatively similar. The symbols show that, in all but the bottom right panel, $M(r) > 1$ on small scales. To estimate the statistical significance of the difference from unity, we have randomized the marks and measured $M(r)$, and then repeated this procedure one hundred times. The solid curve which is close to unity on all scales shows the mean $M(r)$, averaged over these random realizations. The standard deviation around this mean is shown as the dotted line; comparison of the symbols with the shape of this curve suggests that we have weak evidence that close pairs have larger formation redshifts than average.

The bottom right panel appears to behave differently from the others, so a word on why this happens is in order. Notice that this bin contains a much larger range of halo masses. Massive haloes cluster more strongly than low mass ones, so it is plausible that each of the closest pairs in this bin is either a pair of massive haloes, or has one of these massive haloes as one member of the pair. Since massive haloes have, on average, the smallest formation redshifts, $M(r)$ drops on small scales. This again illustrates the complexities of interpretting plots which average over a range of masses.

We have repeated this analysis but using the recaled formation times $\omega_{0.5}$ defined in the previous section. Since this rescaling removes the dependence of formation redshift on mass, we are now allowed to average over the entire range of halo masses when computing the marked correlation function, thus allowing us to increase the signal-to-noise of our measurement. The results are shown in Figure 5; now there is clear evidence that close pairs tend to form earlier than do more distant pairs. At $1h^{-1}$Mpc, for instance, $M_\omega(r) \sim 1.2$; because $M_\omega(r)$ depends on the product of the marks, this suggests that haloes with neighbours on this scale tend to have values of $\omega_{0.5}$ which are typically $\sim 1.2^{0.5}$ times the mean value, but that on scales of order $10h^{-1}$Mpc, this excess is considerably smaller.

The signal appears to be stronger at $z = 0$ than at $z = 0.5$. Some of this is because, as a consequence of the finite mass resolution of the simulations, we do not sample haloes with small values of M/M_* at higher redshifts. It will be interesting to repeat this analysis on simulations with better mass resolution, so as to quantify how the trend with environment depends on M/M_*, and how it depends on redshift (e.g., one might wonder if the signal is clearer at $z = 0$ than at $z = 0.5$ because the correlation with environment shifts to smaller scales at higher redshifts).

4 ALTERNATIVE DEFINITION OF FORMATION

In the previous sections, formation was defined as the first time that at least half the mass of a halo is contained in one progenitor. To illustrate that the trend with environment we find does not depend on this precise definition of formation,

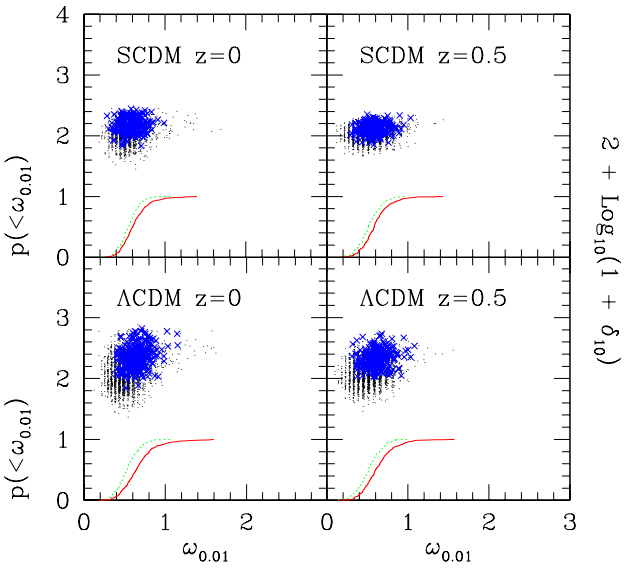

Figure 6. Similar to Figure 2, but now with formation defined as the first time that half the final mass is contained in progenitors which are each more massive than one percent of the parent. Solid and dotted lines show the cumulative formation time distribution for haloes in denser and less dense regions, respectively: Haloes in dense regions tend to have formation times which extend to higher redshifts compared to their counterparts in less dense regions.

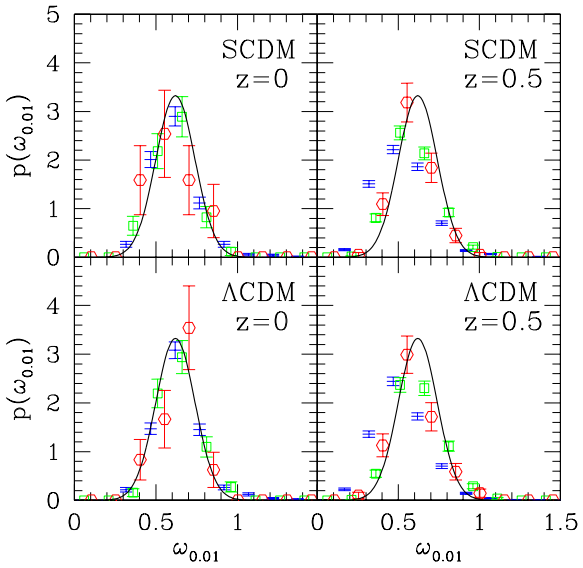

Figure 7. Similar to Figure 3, but now with formation defined as in Figure 6. In this scaled variable, the distribution of formation times is approximately independent of mass. Solid line, drawn to guide the eye, shows a Gaussian distribution with mean 0.62 and rms 0.12.

we have modified the definition as follows: here formation is defined as the first time that at least half the mass of a halo is contained in progenitors each containing at least one percent of the mass of their parent halo. The previous definition corresponds to requiring that the minimum mass of a progenitor be one-half that of the parent. If $z_{0.01}$ denotes this formation time, then $z_{0.01} > z_{0.5}$, but the two formation times depend similarly on halo mass: in both cases, massive haloes form later.

Figure 6 shows the result of rescaling $z_{0.01}$ to $\omega_{0.01}$, similarly to how we rescaled $z_{0.5} \rightarrow \omega_{0.5}$, and then measuring $p(\omega_{0.01})$ in different environments, similarly to what was done in Figure 2. (Figure 7, the analogue of Figure 3, shows that this rescaling removes most of the dependence on the mass of the parent halo mass and the redshift when it virialized.) Figure 6 shows that $p(< \omega_{0.01})$ is shifted towards higher redshifts for the haloes in denser regions (solid curve), indicating that for this definition of formation also, haloes in dense regions form slightly earlier.

In the previous section, we argued that the marked correlation function analysis is a simple and powerful technique for detecting and quantifying environmental dependence. To emphasize this point, Figure 8 shows a marked correlation function analysis using $\omega_{0.01}$ as the mark. Notice how similar this signal is to that shown in Figure 5, in which $\omega_{0.5}$ was used as the mark, and also how much easier it is to see the environmental dependence here, than in Figure 6.

Although we will not pursue this further here, we think it is worth discussing briefly what information we think the shape of the $M(r)$ contains. Suppose we write the weighted correlation function as a bias factor times the unweighted correlation function: $W(r) \approx B^2(r)\,\xi(r)$. In models where environmental effects only matter on small scales, one might reasonably expect this bias factor to become independent of scale on sufficiently large scales. Since $\xi(r)$ typically decreases with increasing separation, the rate at which $M(r) = [1 + B^2\xi(r)]/[1 + \xi(r)] \rightarrow 1$ on large scales

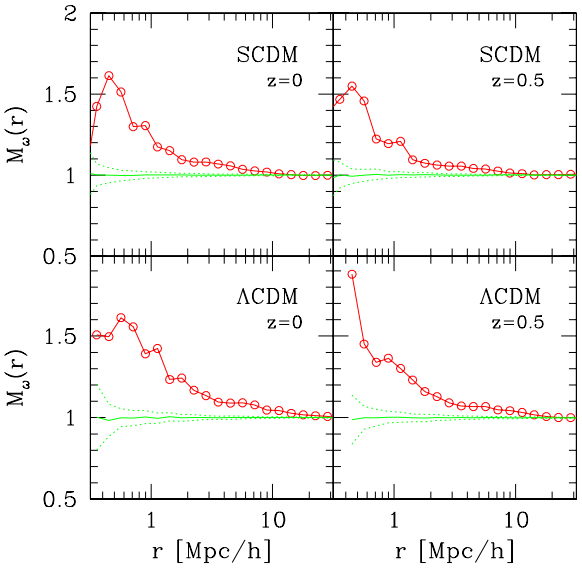

Figure 8. Similar to Figure 5, but now with formation defined as the first time that half the final mass is contained in progenitors which are each more massive than one percent of the parent.

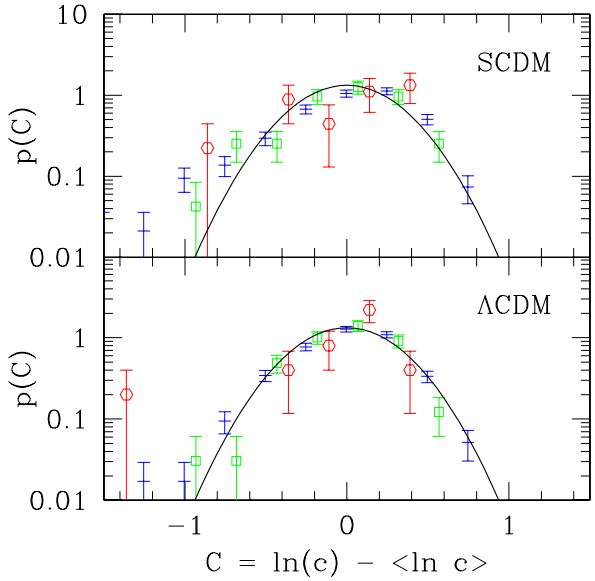

Figure 9. Scaled distribution of halo concentrations at $z = 0$. Bars, squares and hexagons show results for halos with masses in the range $1 < M/M_* \leq 2$, $4 < M/M_* \leq 8$, and $16 < M/M_* \leq 32$. In this scaled variable, the distribution of halo concentrations is approximately independent of mass. Solid line shows that this shape is well approximated by a Lognormal with rms $\sigma_{\ln c} = 0.3$.

is determined by the bias factor. This suggests a generalization of the test we have performed: smooth the marked field (e.g., compute the mean formation time in spheres of radius R), compute the correlation function of the smoothed marked field, and normalize by the correlation function of the smoothed density field. If the mark is determined by local effects, then a measurement of the shape of the marked correlation function on large smoothing scales is a measurement of the bias associated with the mark.

5 DISCUSSION

We presented evidence that halo formation is weakly correlated with the surrounding density field. The weakness of the correlation suggests that the usual excursion set model neglect of correlations is a good approximation, but the fact that a correlation does exist means that, as the available data on galaxy properties and the surrounding large scale structure becomes more precise, it will become necessary to build a more sophisticated model.

Our demonstration that environmental effects do leave a mark on the halo population, and that marked correlation functions are a useful method of detecting and quantifying this, suggests that a marked correlation analysis of halo concentrations, spins, shapes and alignments should yield interesting results. For instance, the particular definition of halo formation we chose to study in Section 4 is motivated by the work of Navarro, Frenk & White (1997) who argue that $z_{0.01}$ correlates strongly with the central concentration of the parent halo. Since our analysis indicates that halo formation

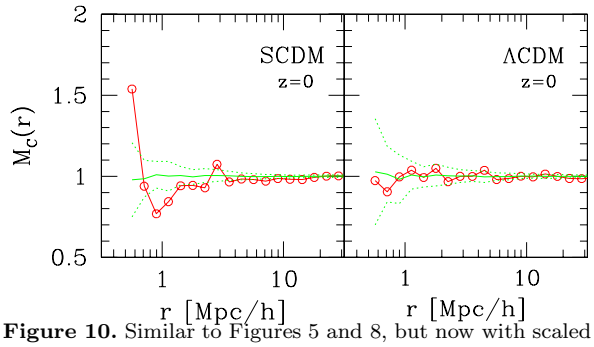

Figure 10. Similar to Figures 5 and 8, but now with scaled concentration C as the mark. There is no evidence that, once mass dependent trends have been removed, halo concentrations depend on environment. It will be interesting to see if this conclusion remains when this analysis is repeated with higher resolution simulations.

depends on environment, it is plausible that the structural properties of haloes will also depend on environment.

As a first step, we have attempted a measurement which uses the halo concentration as the mark. This is not entirely straightforward, because the GIF simulations we have used in this paper do not have particularly good mass-resolution, so they are not well suited to estimating the density run around halo centres; as a result, the halo concentrations we estimate are rather noisy. Nevertheless, if we select a sample for which the Navarro et al. formula is a better fit, then we find reasonable agreement with previous higher resolution studies (e.g. Jing 2000) which were restricted to considerably smaller halo samples. Specifically, we find that on average, massive halos have slightly smaller concentration parameters: $\langle \ln c \rangle = \ln[c_* \, (M/M_*)^{-0.1}]$, with $c_* = 8$ and 9 at $z = 0$ in the SCDM and ΛCDM runs. More importantly, the distribution around the mean concentration is approximately independent of halo mass, and is well approximated by a lognormal with rms $\sigma_{\ln c} = 0.3$. This is shown in Figure 9.

Because the same lognormal shape provides a good description of the distribution of concentrations at all masses, we can use it to remove mass-dependent trends, as we did in our study of halo formation in main text. Figure 10 shows a marked correlation function in which this scaled concentration was used as the mark. There is no evidence that the concentrations of close pairs are any different than those of more widely separated pairs, suggesting that, once mass-dependent trends have been removed, halo concentrations do not depend on environment. Since this strongly suggests that the connection between halo formation and concentration is not as straightforward as is generally assumed, it will be interesting to see if this conclusion remains when the analysis is repeated on higher resolution simulations.

Although we believe a marked correlation analysis of halo concentrations, spins, shapes and alignments will yield interesting results, we think that there is one measurement which is more interesting still. Recent studies of pure dark-matter simulations suggest that galaxies are likely associated with the substructure components of dark matter haloes (Kravtsov et al. 2003). A marked correlation correlation analysis which uses the number of subclumps as the mark would be extremely interesting, because one of the crucial assumptions in current interpretations of the galaxy corre-

lation function is that the number of galaxies which form in a halo depends on halo mass, but does not depend on halo environment. For similar reasons, a marked correlation analysis of the sites in which gas cools in dark-matter plus hydro- simulations will be very interesting, particularly in view of the fact that conventional tests find little evidence for environmental trends (Berlind et al. 2003).

Finally, it is worth mentioning that models based on the work of Efstathiou & Rees (1988) which relate the formation of massive black holes to halo formation assume that, at fixed mass, the clustering of halos is independent of whether or not they formed recently. Measurements in simulations of the large-scale clustering of merger sites indicate that, on scales larger than a few Mpc, this assumption is accurate (Percival et al. 2003). Similarly, simulations show that the large-scale cross-correlation between halos that formed recently and the entire halo population is similar to the auto-correlation function of the entire halo population (Kauffmann & Haehnelt 2002). Both measurements indicate that, at least on large scales, the only trends with environment are those which arise from the correlation between mass and environment, consistent with the simplest excursion set prediction.

Although they emphasized what they saw on large scales, on smaller scales both Kauffmann & Haehnelt (2002) and Percival et al. (2003) do see weak evidence for small additional trends with environment. Their measurements can be reconciled with the excursion set approach if we recall that the excursion set prediction is based on the assumption that different scales are uncorrelated—in the jargon, this comes from using a smoothing filter which is sharp in k-space. The predictions of the excursion set approach do depend on the choice of filter. However, the precise choice of filter cannot matter on scales larger than the correlation length. Thus, the predicted importance of halo mass rather than environment *on large scales*, although it is derived from consideration of the sharp k-space filter, is a generic prediction of the approach. On the other hand, one does expect filter-dependent environmental trends on smaller scales. Since the sharp k-space filter is not expected to be a reasonable choice on small scales, one generically expects to find correlations with environment on small scales (over and above those associated with halo mass). Presumably, it is these correlations which our analysis is well-suited to detecting.

We would like to thank the Aspen Center for Physics for support, and for providing the stimulating environment in which this work was begun. We would also like to thank the Virgo consortium for making the simulation data used here publically available at `http://www.mpa-garching.mpg.de/Virgo`, and Andy Connolly, Bob Nichol and the other members of the Pittsburgh Computational Astrostatistics (PiCA) Group for providing a fast code with which to evaluate marked correlation functions. This work was supported by NASA grant NAG5-13270, and by an FR Type II Grant from the University of Pittsburgh.

REFERENCES

Berlind A. A., Weinberg D. H., Benson A. J., Baugh C. M., Cole S., Davé R., Frenk C. S., Jenkins A., Katz N., Cedric G., 2003, ApJ, 593, 1
Bond J. R., Cole S., Efstathiou G., Kaiser N., 1991, ApJ, 379, 440
Efstathiou G., Rees M J., 1988, MNRAS, 230, 5P
Epstein R., 1983, MNRAS, 205, 207
Frenk C. S., Colberg J. M. Couchman H. M. P., et al., 2000, astro-ph/0007362
Jing Y. P., 2000, ApJ, 535, 30
Kauffmann G., Colberg J. M., Diaferio A., White S. D. M., 1999, MNRAS, 303, 188
Kauffmann G., Haehnelt M., 2002, MNRAS, 332, 526
Kravtsov A., et al. 2003, ApJ, submitted (astro-ph/0308519)
Lacey C., Cole S., 1993, MNRAS, 262, 627
Lemson G., Kauffmann G., 1999, MNRAS, 302, 111
Mo H. J., White S. D. M., 1996, MNRAS, 282, 347
Navarro J., Frenk C., White S. D. M., 1997, ApJ, 490, 493
Nusser A., Sheth R. K., 1999, MNRAS, 303, 685
Peebles J. E. P., 1993, Principles of Physical Cosmology, Princeton Univ. Press, Princeton, NJ
Percival W. J., Scott D., Peacock J. A., Dunlop J. S., 2003, MNRAS, 338, 31P
Sheth R. K., Tormen G., 1999, MNRAS, 308, 119
Sheth R. K., Mo H. J., Tormen G., 2001, MNRAS, 323, 1
Sheth R. K., Tormen G., 2002, MNRAS, 329, 61
Sheth R. K., Tormen G., 2004, MNRAS, in press (astro-ph/0402055)
White S. D. M., 1996, in Cosmology and Large Scale Structure, Les Houches Session LX, eds. R. Schaefer, J. Silk, M. Spiro, and J. Zinn-Justin, Elsevier, Amsterdam, p. 349